

Article

# Analyzing the operation of a hybrid photovoltaic-diesel-generator-grid hybrid microsystem—Case study

Elisabeta Spunei<sup>1,\*</sup>, Naomi-Ionela Soanda<sup>1</sup>, Mihaela Martin<sup>2,\*</sup>, Gheorghe Stefan Matasaru<sup>3</sup><sup>1</sup> Department of Engineering Sciences, Faculty of Engineering, Babes-Bolyai University, 400028 Cluj-Napoca, Romania<sup>2</sup> Department of Public Administration and Management, Faculty of Political, Administrative and Communication Sciences, Babes-Bolyai University, 400028 Cluj-Napoca, Romania<sup>3</sup> Endress Zenesis Group Romania SRL, 325300 Bocsa, Romania\* **Corresponding authors:** Elisabeta Spunei, [elisabeta.spunei@ubbcluj.ro](mailto:elisabeta.spunei@ubbcluj.ro); Mihaela Martin, [mihaela.martin@ubbcluj.ro](mailto:mihaela.martin@ubbcluj.ro)

## CITATION

Spunei E, Soanda NI, Martin M, Matasaru GS. (2024). Analyzing the operation of a hybrid photovoltaic-diesel-generator-grid hybrid microsystem—Case study. *Journal of Infrastructure, Policy and Development*. 8(9): 7777. <https://doi.org/10.24294/jipd.v8i9.7777>

## ARTICLE INFO

Received: 4 July 2024

Accepted: 16 July 2024

Available online: 4 September 2024

## COPYRIGHT



Copyright © 2024 by author(s).

*Journal of Infrastructure, Policy and Development* is published by EnPress Publisher, LLC. This work is licensed under the Creative Commons Attribution (CC BY) license. <https://creativecommons.org/licenses/by/4.0/>

**Abstract:** The scientific objective of this study is to demonstrate how a hybrid photovoltaic-grid-generator microsystem responds under transient regime to varying loads and grid disconnection/reconnection. The object of the research was realized by acquiring the electrical magnitudes from the three PV systems (25 kW, 40 kW, and 60 kW) connected to the grid and the consumer (on-grid), during the technological process where the load fluctuated uncontrollably. Similar recordings were also made for the transient regime caused by the grid disconnection, diesel generator activation (450 kVA), its synchronization with PV systems, power supply to receivers, and grid voltage restoration after diesel generator shutdown. Analysis of the data focused on power supply continuity, voltage stability, and frequency variations. Findings indicated that on-grid photovoltaic systems had a 7.9% maximum voltage deviation from the standard value (230 V) and a frequency variation within  $\pm 1\%$ . In the transient period caused by the grid disconnection and reconnection, a brief period with supply interruption was noted. This study contributes to the understanding of hybrid system behavior during transient regimes.

**Keywords:** hybrid plant; photovoltaic system; diesel-generator set; acquisitions of electrical size; waveforms; voltage; frequency

## 1. Introduction

Hybrid power plants that have emerged recently combine various renewable energy sources and can be linked to the grid, along with energy storage systems or diesel generators (Huang and Bao, 2016; Kemp et al., 2023). To guarantee the power needs and correct functionality of these systems, it is essential to establish the experimental load curve (Brahim, 2019). Energy storage systems like batteries or hydrogen enable the coverage of peak loads or contribute to meeting energy demands in the absence of renewable sources (Badea et al., 2016; Das et al., 2024). Hence the benefit of these hybrid systems combined with storage systems in increasing the variability of energy production (Hasan, 2023). Another important benefit resulting from the utilization of renewable sources is the decrease in electricity expenses, particularly through various programs offered by state authorities (Atanasoae et al., 2019; Babatunde et al., 2020). At the same time, the use of renewable energy sources leads to a decline in carbon emissions, contributing to reduced pollution and improving public health (Khosravani et al., 2023).

While grid-connected photovoltaic systems have demonstrated their dependability and effectiveness in supplying electricity, they are rendered inactive

during grid failures, causing inconvenience to consumers. This issue is addressed by employing hybrid systems that eliminate the disturbance caused by grid voltage loss and ensure uninterrupted power supply to consumers (Mthwecu et al., 2015). Consequently, despite the distinct features of each energy source, they can work together to meet the energy demand based on the load requirement (Dehghani et al., 2023). Studies indicate that these combined systems have unique interactions with the grid compared to individual systems (Kemp et al., 2023; Pan et al., 2009). For instance, a study conducted in South Africa materialized by measurements on a hybrid PV-diesel generator microgrid, found dynamic changes in the supply voltage (Maritz et al., 2024). This highlights the importance of maintaining power quality (Chindris et al., 2016; Liviu et al., 2018) when dealing with variable loads and distributed power generation.

Various simulation programs have been developed to analyze the steady-state and dynamic operation of a hybrid plant, estimating the system's behavior and its impact on the power grid or consumers under different disturbance scenarios (Siddaraj and Tangi, 2016). Thus, a simulation program was created in Matlab/Simulink for a hybrid wind-hydroelectric system connected to the power grid. For dynamic operations it was observed that the power grid can ensure stability of the grid-connected hybrid power plant at varying wind speeds (Huang and Bao, 2016). Simulations were also conducted to assess the steady-state and dynamic performance of a hybrid photovoltaic-wind power system under constant wind speeds, different temperature values, and solar irradiance levels (Martínez and Medina, 2010). Simulation results from the dedicated software Homer for a hybrid photovoltaic-diesel generator-battery system showed efficiency in various economic, environmental, and technical scenarios, reducing energy storage needs (Halabi et al., 2017). Due to changing weather conditions, the output power of the PV system fluctuates, leading to frequency variations, which can be mitigated by implementing a storage system (Nguyen et al., 2021). Results from the operation simulation show that utilizing a fuzzy controller for frequency control enables the PV system to function at its peak power efficiency (Manoj et al., 2011).

Simulation models were utilized in the context of a cascaded hydroelectric-photovoltaic hybrid system to enable the attainment of an efficient operating approach that facilitates the reduction of peak loads. The analysis of the load variation mode served as the foundation for this strategy. Upon the implementation of this strategy, its feasibility was demonstrated (Zhang et al., 2021).

While numerous papers present the simulation results of hybrid systems' steady-state and dynamic operation regarding power quality and system stability (Pan et al., 2009), few discuss conclusions drawn from field measurement analysis demonstrating the operations of such installations.

In a PV-hydro-solar hybrid system with an energy storage system application, the output voltages of individual components were measured and determined to remain relatively stable despite load variations (Ratnata et al., 2019). Different techniques of inverter control are utilized to guarantee output voltage stability (Isakov and Todorovic, 2021) and the proper operation of the entire system in normal operating conditions and grid voltage imbalances. The operation of grid-connected hybrid systems can face challenges due to harmonics impacting power quality. Therefore, for proper operation of the whole system, conducting measurements is essential to identify

solutions that minimize adverse effects on the power grid (Averbukh et al., 2018; Giraud and Salameh, 2007).

Degradation/aging of certain components is among the issues that arise during the operation of these systems. A suggestion has been made to utilize a model that considers load variations to determine and forecast the components needing replacement (Ameen et al., 2015).

The paper presents the analysis of a hybrid microsystem comprising three photovoltaic systems of varying powers (25 kW, 40 kW, 60 kW), a 450 kVA diesel generator set, the power grid, and an industrial consumer with fluctuating load. Chapter 1 presents the usefulness of hybrid power generation systems, simulation of various system setups, and the challenges encountered during their operation. Chapter 2 presents the hybrid microsystem and flow diagram utilized in the analysis. The PV systems, diesel generator, consumer, and grid power mode's technical characteristics are outlined. Additionally, the interconnection scheme of the systems is displayed through the lux diagram, which serves as the basis for the analysis. Moving on to chapter 3, the functionality of the three on-grid photovoltaic systems is explained, relying on measurements conducted using a grid analyzer set at a sampling frequency of 200 kHz. By examining the voltage, current, frequency, and power waveforms, the fluctuations in voltage, frequency, and power continuity for the consumer under variable and uncontrollable loads are identified. The recorded values were analyzed to ensure compliance with quality standards. Chapter 4 presents the operation of the hybrid plant during the transient regime of grid disconnection and reconnection. The analysis utilized electrical data obtained from the network analyzer and the resulting waveforms. The transient process involved the grid voltage disappearing and the diesel generator automatically switching on, leading to synchronization with the photovoltaic systems and providing power to the consumer. Another examined transient regime was when the grid voltage reappeared, causing the generator to stop operating and the PV systems to synchronize with the grid, supplying the consumer accordingly. In chapter 5, we have outlined the conclusions derived from the conducted research. It was discovered that the voltages provided by the photovoltaic systems exceed the specified range in the regulations. Additionally, the analysis revealed that power supply continuity is maintained and the voltage frequency remains within the defined limits. Measurements taken during transient regimes caused by grid disconnection and reconnection, as well as during operation in the diesel generator-photovoltaic systems-consumer setup, demonstrated the stable operation of the hybrid system, with voltage and frequency values adhering to the set limits. A brief moment occurred where the consumer experienced a one-second power loss due to generator set connection and disconnection. This underscores the importance of thoroughly examining the performance of hybrid systems in various transient regimes, especially for critical receivers, to ensure compliance with quality power supply standards. The research will continue towards identifying and implementing solutions that guarantee uninterrupted power supply while meeting the necessary electricity quality standards.

## **2. Hybrid microsystem and flow diagram**

The hybrid system analyzed is atypical because it supplies power to a user who

creates prototypes of mechanical, electrical, or combined products. It lacks electrical machinery that operates continuously, dealing with highly variable and uncontrolled loads. The operational conditions of the various equipment pieces differ significantly from day to day. Consequently, the measured experimental load profiles/curves measured daily or monthly, vary greatly, necessitating an assessment of the hybrid system's performance to ensure it meets the required electricity supply standards. Another point to emphasize the unique nature of the consumer is its positioning at the tail end of the electricity distribution network. This results in lower voltage levels during peak network usage. Additionally, frequent power outages from the main grid can disrupt production and render PV systems non-functional. To guarantee uninterrupted power supply, a diesel-generator set was used to complement the grid and synchronize with the photovoltaic systems. After implementing the synchronization scheme for the photovoltaic systems with the diesel-generator set and the automatic transition to the grid (at voltage emergence), the resynchronization of the PV with the grid was observed, and the behavior of the hybrid system during transient regimes was studied.

The hybrid plant is described as a system providing power to an industrial consumer, comprising the power grid, three photovoltaic systems of varying capacities, and a diesel generator set. A three-phase transformer connected to the 20 kV grid supplies a standardized 400 V three-phase voltage in the secondary. The power supply block diagram of the industrial consumer is illustrated in **Figure 1**, revealing that the receivers are connected to three separate circuits.

The photovoltaic system is made up of three distinct systems that were installed at different times, each having specific technical characteristics:

- A 60 kW photovoltaic system (PV1) consisting of 126 photovoltaic panels with a capacity of 530 W and two 30 kW inverters;
- A 25 kW photovoltaic system (PV2) consisting of 48 PV panels with a power of 530 W and one 30 kW inverter, similar in configuration to the 60 kW system;
- A 40 kW PV system (PV3) consisting of 160 PV panels with a power of 270 W each and 2 inverters of 20 kW (Spunei et al., 2021; Spunei et al., 2022).

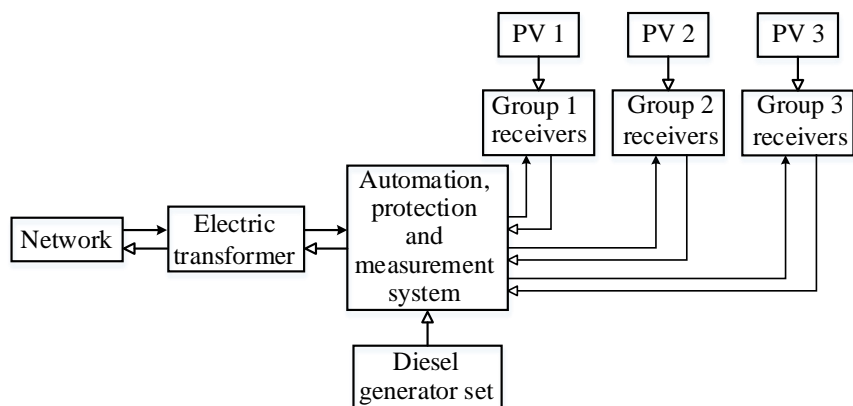


**Figure 1.** Block diagram of the hybrid installation (grid-photovoltaic system-diesel-generator set) supplying the industrial consumer.

The inverters used are on-grid inverters, necessitating details about the presence

of the supply voltage and synchronized pulses for the PV system to function. The final part of the PV system was activated in March 2023, with the consumer transitioning into a prosumer as well.

In times of unavailability of the PV system and absence of grid supply, the diesel generator set supplies electricity. Moreover, in case of a drop in grid voltage, the automation scheme manages the diesel generator set to activate and synchronize with the PV system. It was essential for the PV system to ensure electricity supply in the absence of grid voltage. The diesel generator has a power of 360 kW (450 kVA), running at 1500 rpm and providing standard single-phase and three-phase voltage at 50 Hz. The excitation system of the synchronous generator includes an electronic setup managed by a specialized microprocessor module for regulation, control, and monitoring.

The industrial consumer's receivers have an installed capacity of 230 kW, distributed as follows:

- 35 kW for receiver group 1, which includes an electrostatic painting installation along with the lighting system and various low-power equipment.
- 155 kW for group 2, consisting of receptors similar to those in hall 1, including an electrostatic painting plant, a laser cutting plant for metal materials, a plant for bending metal parts (abkant), a welding plant, and a crane.
- 40 kW for group 3 receptors, which include a crane along with the lighting system and various low-power equipment.

From the information gathered from the prosumer's metering system, it was discovered that throughout a year, the entire PV system provided 32.31% of the energy used by the industrial consumer. Due to no production activities occurring at the industrial site during the weekend, the energy generated by the PV system was transferred to the grid, representing 15.1% of the electricity consumption. Analyzing the total electricity generated by the PV system in relation to the user's total consumption it was found that this represented 42.21%, meaning the PV system met approximately half of the consumer's electricity demands.

In **Figure 2** we have shown the flow diagram used for analyzing the operation of the hybrid photovoltaic-diesel-generator microsystem.

After setting up the grid analyzer, it is essential to acquire the electrical quantities at the output of the inverters from the photovoltaic systems interconnected with the grid and the consumer (with variable and uncontrollable load) from the automation, protection, and metering panel. The main goal is to ensure a continuous power supply. Failure to meet this requirement will necessitate checking the diesel-generator set and configuring it to quickly activate when the main voltage decreases or disappears. Two other requirements to be assessed relate to the voltage and frequency levels provided, even in critical situations resulting from the simultaneous connection of multiple high-power receivers and transient regimes. If these criteria are not met, adjustments must be made to the inverters, diesel generator, or there should be a limitation on the concurrently connected loads.

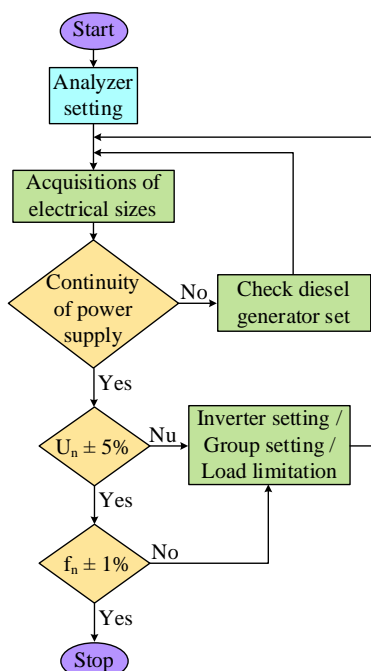


**Figure 2.** Flow diagram used in the analysis.

The main advantages determined by the implementation of the proposed model are:

- Ensuring continuity in steady-state and transient regime power supply determined by large and uncontrolled load variations;
- Ensuring uninterrupted power supply during transient regimes caused by disconnection and reconnection of the grid, or by diesel-generator set start-up and shutdown.

Ensuring the appropriate voltage and frequency level in the case of steady state and transient regimes caused by load variations, synchronization and desynchronization of photovoltaic installations, grid disconnections and reconnections, automatic diesel generator entry and shutdown.

### 3. Analysis of the operation of the photovoltaic system in on-grid operation

To assess the efficiency of photovoltaic systems in both on-grid and variable load scenarios, the variations in voltages, currents, and frequency were carefully examined. Analysis involved identifying minimum, maximum, and average values, calculating deviations, and then comparing the results against the standards' specified limits.

The measurements were conducted using a Fluke 435 network analyzer, which adheres to IEC 61000-4-30 (IEC, 2015), complies with the EN50160 power quality standard (EN, 1999), and can display ten power quality parameters simultaneously on its screen (Fluke, 2024). The device used has a measurement class A, an accuracy of 0.1% of nominal voltage, and a sampling rate of 200 kHz per channel.

Recordings were taken for every PV system for a duration of 2 h (IEC, 2015), while the analyzer was positioned at the output of the inverters. The voltage, current, power, frequency, and power factor waveforms were examined in the data. Other

parameters such as power interruptions, voltage sags, and harmonics have been examined as well, although this paper focuses only on the analysis of voltage and frequency fluctuations. A comparison was made between the minimum and maximum values and the reference values specified in the standards. Simultaneously, the deviations from these reference values were assessed to ascertain if they fell within the specified limits.

The following quality indicators were also calculated for each analyzed case:

- Frequency deviation  $\Delta f$ :

$$\Delta f = f_n - f \quad (1)$$

where  $f_n$  represents the nominal frequency value and  $f$  represents the actual frequency;

- Relative frequency deviation  $\varepsilon f$ :

$$\varepsilon_f [\%] = \frac{f - f_n}{f_n} \cdot 100 \quad (2)$$

- Relative voltage deviation  $\varepsilon U$ :

$$\varepsilon_U [\%] = \frac{U_f - U_{f_n}}{U_{f_n}} \cdot 100 \quad (3)$$

where  $U_f$  is the phase voltage value and  $U_{f_n}$  is the nominal phase voltage value.

### 3.1. Analysis of the operation of the 25 kW grid-connected PV system with variable and uncontrollable load

Recordings were taken on 29 April 2024, between 11:11 and 13:11, for the 25 kW PV system. The variation of the supplied phase voltages is illustrated in **Figure 3**. The maximum values are depicted in red, while the minimum values are shown in blue.

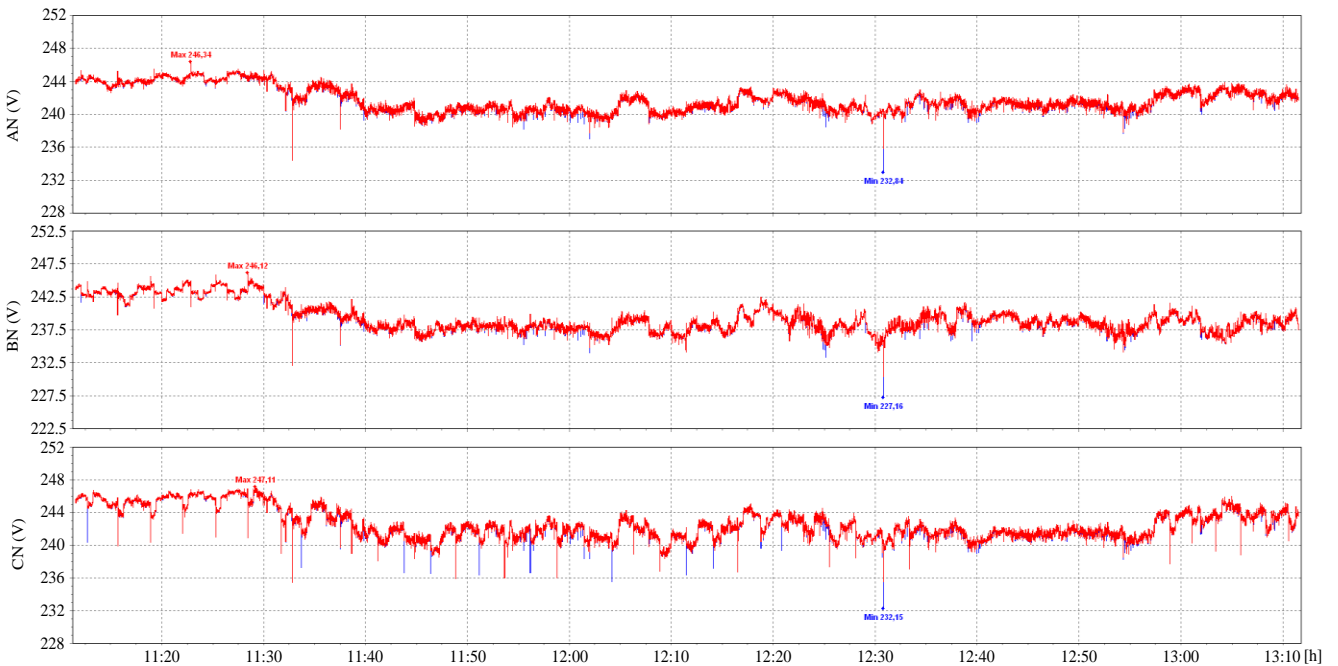


**Figure 3.** The variation mode of the phase voltages provided by the 25 kW PV system.

The analysis shows that the *R* and *T* phase voltages' minimum values exceed the Romanian standard of 230 V (ANRE, 2021). Within **Table 1**, we detail the minimum and maximum phase voltage values recorded, along with the percentage deviation

from the standard value.

**Table 1.** Electrical values measured on the 25 kW PV system.

Measured electrical size	Phase R/General			Phase S			Phase T		
	Min.	Max.	$\varepsilon_U\%$	Min.	Max.	$\varepsilon_U\%$	Min.	Max.	$\varepsilon_U\%$
Phase voltage [V]	232.8	246.3	+7.1	227.2	246.1	-1.2/ +7	232.2	247.1	+7.4
Phase currents [A]	4	26.3	-	4.3	26.6	-	4.1	26.2	-
Frequency	49.957	50.065	$\varepsilon_f$ -0.086%/+ 0.13%						

According to Romanian regulations (ANRE, 2021), 95% of the actual voltage values in the boundary well, averaged over 10 minutes, should not deviate more than +5%/-10% from the nominal voltage. Based on the data from the measuring equipment, it was observed that the average voltage values were as follows: phase R—241.8 V, phase S—239.3 V, phase T—242.6 V. 95% of the actual values, averaged over a 10-minute interval, were: phase R—244.6 V (+6.3%), phase S—243.8 V (+6%), phase T—246.1 V (+7%). In conclusion, the phase voltage values from the 25 kW PV system do not comply with the electricity supply quality requirements, the relative deviations being greater than  $\pm 5\%$ .

From analyzing the fluctuations in current throughout the observed timeframe, depicted in **Figure 4**, it was discovered that the currents exhibit symmetry, albeit with a difference of 22 A between the highest and lowest values documented. The use of single-phase receivers results in a slight asymmetry of the currents, leading to an unbalanced loading of the three phases and a slight asymmetry of the voltages. The current’s peak and trough values for each of the three phases are detailed in **Table 1**.

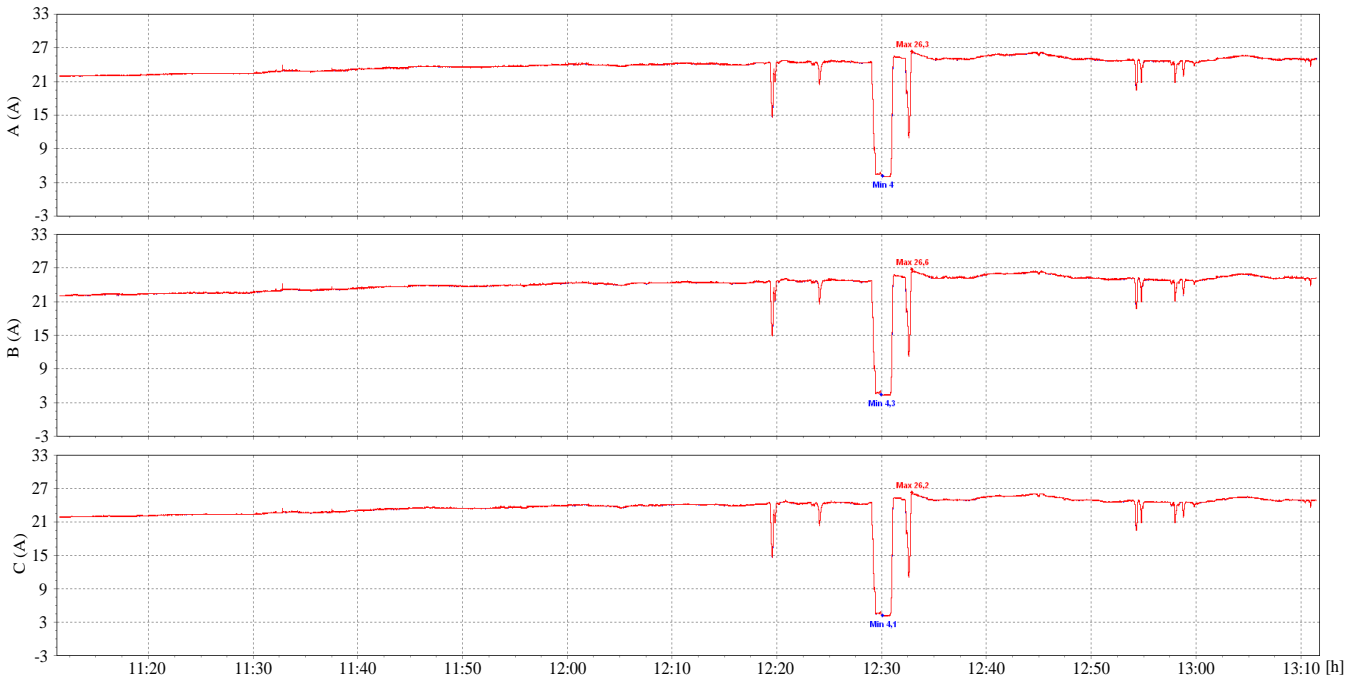


**Figure 4.** The variation mode of the currents in the three power phases of the 25 kW PV system.

In **Figure 5** we have shown the active power’s fluctuation during the analyzed period. The range observed is from a minimum of 2.88 kW to a maximum of 18.87



kW. Throughout the recorded period, the system supplied a maximum power equal to 75% of the PV system's installed power.

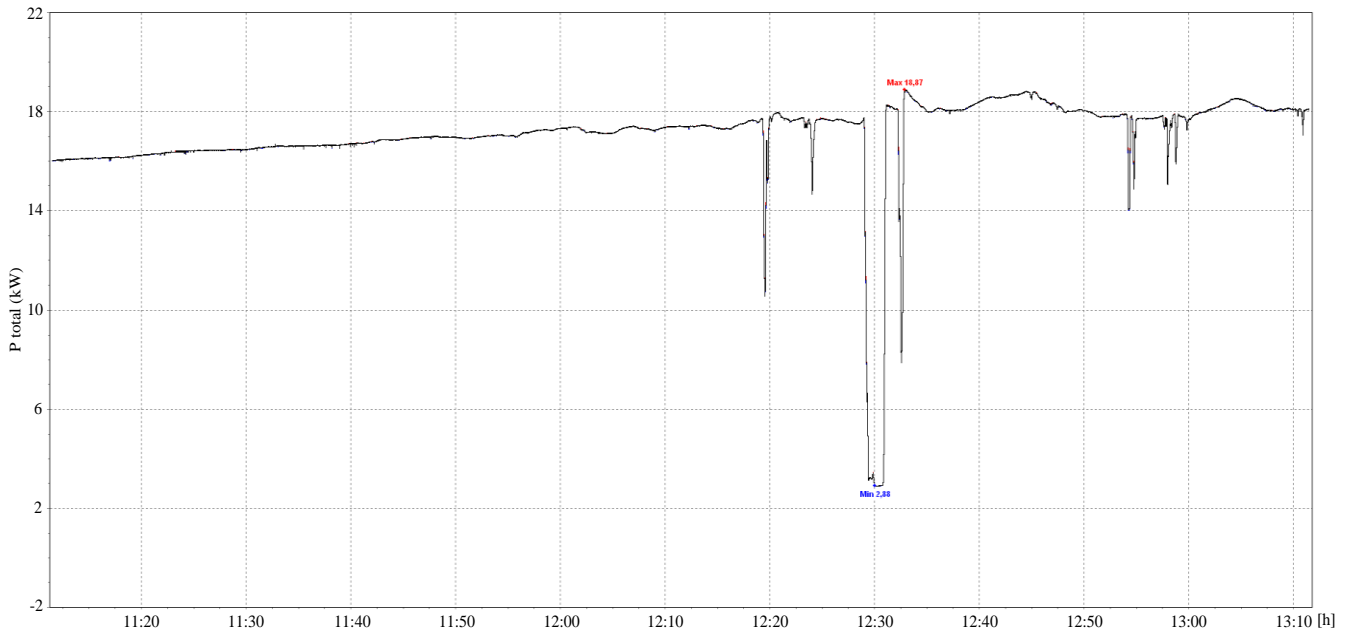


**Figure 5.** The variation mode of the power supplied by the 25 kW PV system.

From the recordings, we have also determined the mode of frequency variation. In **Table 1**, we have recorded the extreme values and the deviation from the standardized value of 50 Hz. The standards in Romania mention that the normalized limits of frequency variation are  $\pm 1\%$  (ANRE, 2021). By examining the shape of the frequency variation in **Figure 6**, a significant variation is observed. However, an analysis of the measured values reveals that it falls within the permissible range of variation.

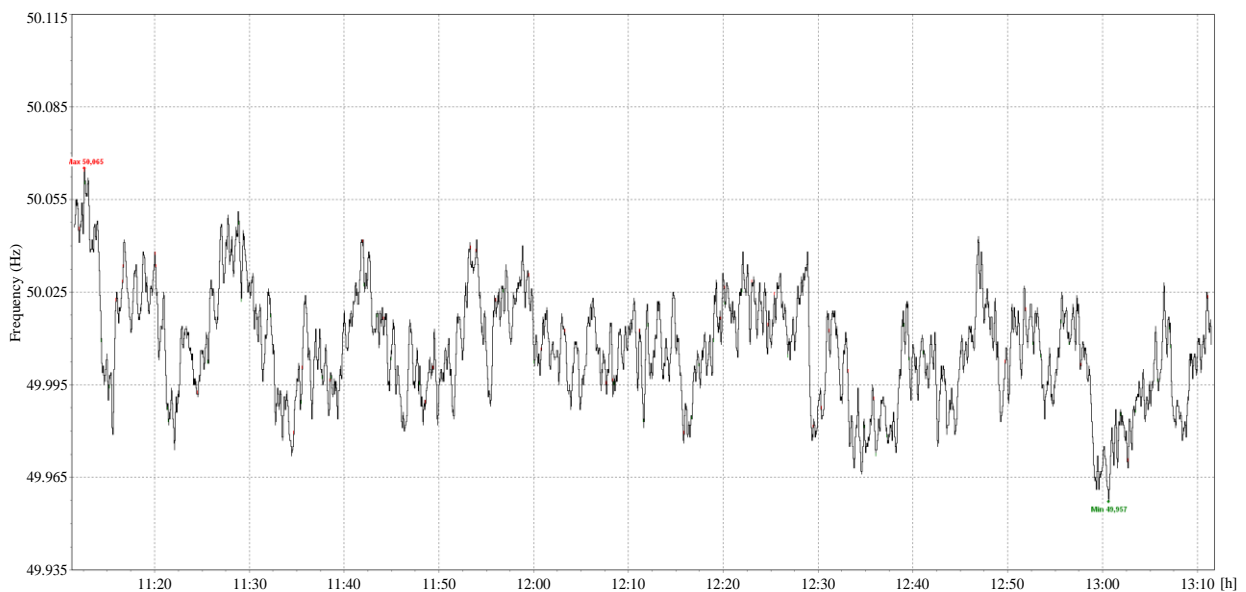


**Figure 6.** The variation mode of the power supplied by the 25 kW PV system.

The measurement system enabled the assessment of the power factor and PF,

considering the deforming power's value. The measurements revealed a  $\cos\phi$  value of 1 and a minimum PF value of 0.95, indicating the absence of reactive power in this system, thus avoiding extra expenses.

### 3.2. Analysis of the operation of the 40 kW grid-connected PV system with variable and uncontrollable load

For analyzing the electrical parameters of the 40 kW PV system, we utilized the same grid analyzer and conducted the measurements within the time frame of 13:35 ÷ 15:35 on the same day. **Figure 7** illustrates the fluctuation pattern of the phase voltages supplied by the 40 kW PV system, highlighting both the minimum and maximum values. These values, along with their deviation from the standardized value, are detailed in **Table 2**. It is evident in this scenario that all the minimum phase voltage values exceed the standardized value.

**Table 2.** Electrical values measured on the 40 kW PV system.

Measured electrical size	Phase R/General			Phase S			Phase T		
	Min.	Max.	$\varepsilon U\%$	Min.	Max.	$\varepsilon U\%$	Min.	Max.	$\varepsilon U\%$
Phase voltage [V]	237.2	246.1	+6.96	238.1	246.8	+7.3	239.8	248.2	+7.9
Phase currents [A]	8.5	42.7	-	8.7	42.9	-	8.6	42.3	-
Frequency	49.937	50.035	$\varepsilon f: -0.126\% / +0.07\%$						

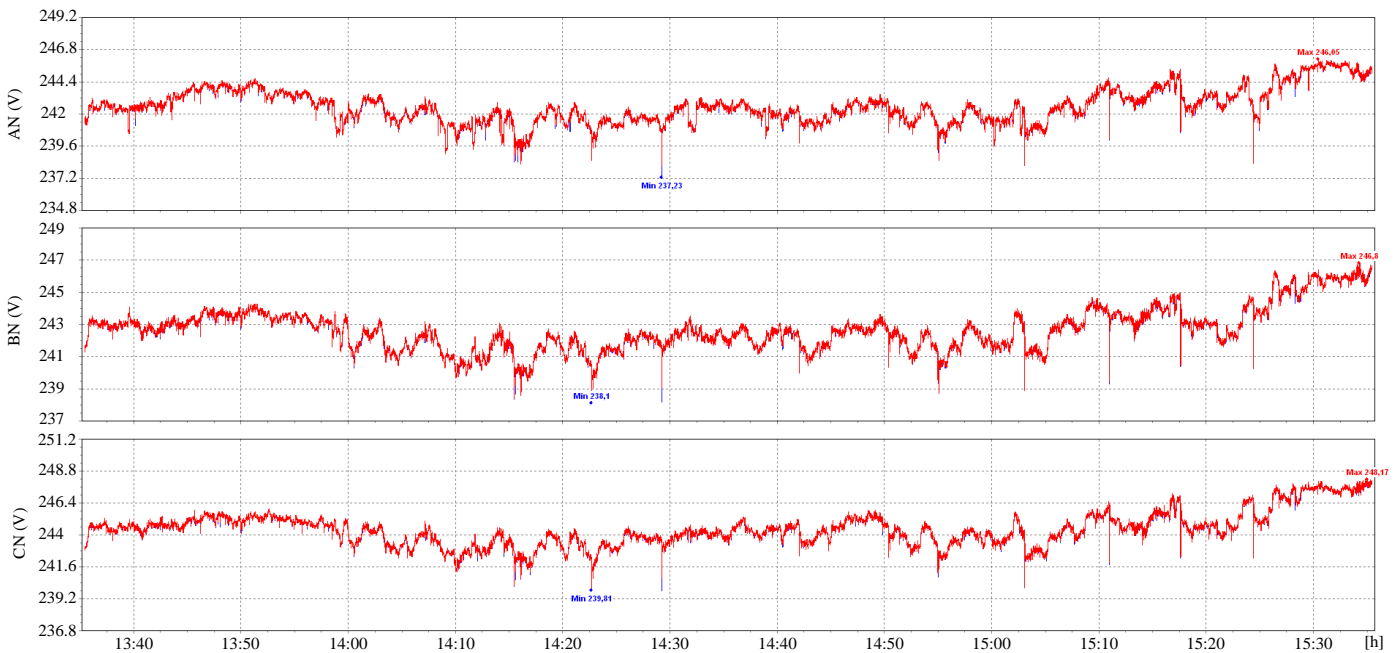


**Figure 7.** The variation mode of the phase voltages provided by the 40 kW PV system.

For this PV system, the mean voltages for each phase were as follows: 242.6 V on R phase, 242.7 V on S phase, and 244.4 V on T phase. When examining the 10-minute average phase voltages, 95% of the measured values were: 245.1 V on R phase (+6.6%), 245.6 V on S phase (+6.8%), and 247.3 V on T phase (+7.5%). Ultimately, the phase voltage values from the 40 kW PV system fail to meet the electricity quality standards, the relative deviations being greater than  $\pm 5\%$ .

In relation to the fluctuations in the currents illustrated in **Figure 8**, it was observed that they exhibit substantial variations, yet are nearly symmetrical. The **Table 2** displays the minimum and maximum current values for the three phases.

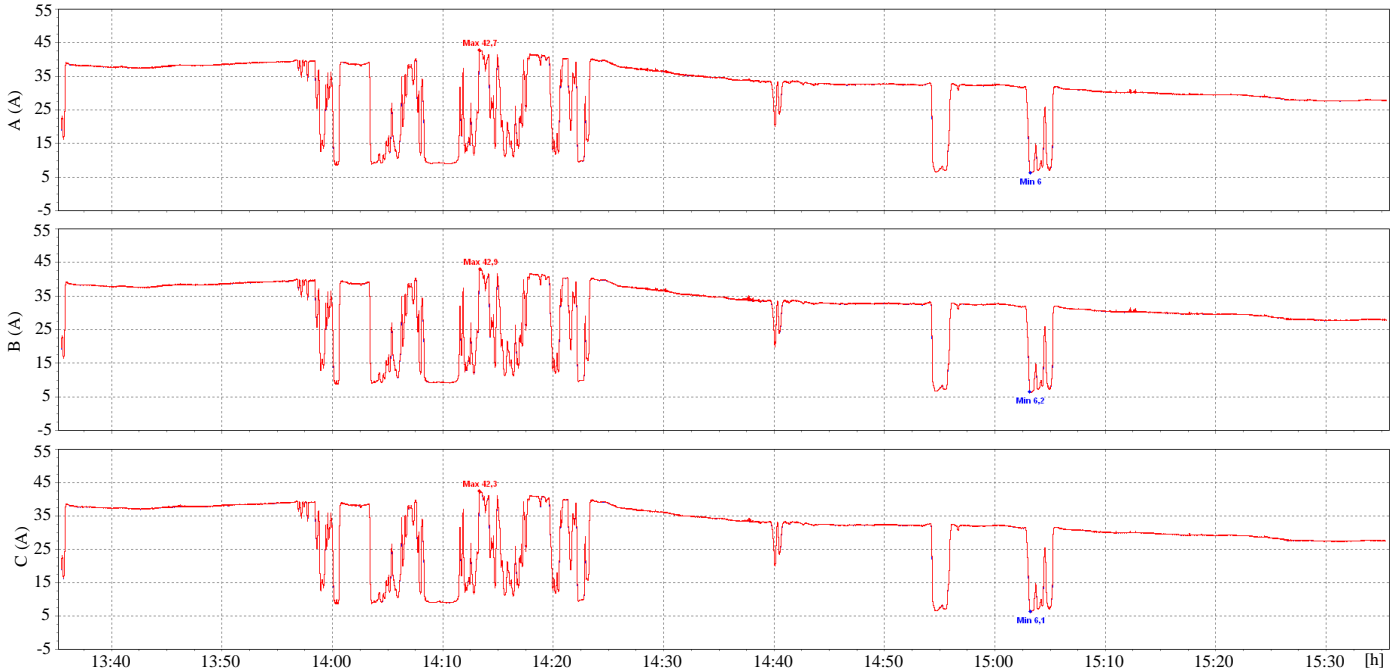


**Figure 8.** The variation mode of the currents in the three feed phases of the 40 kW PV system.

**Figure 9** illustrates the fluctuation of power provided by the 40 kW PV system. It demonstrates a range of 4.32 kW to 30.9 kW. The peak power supplied accounts for 77.25% of the total installed power of the PV system. The system had a power factor ( $\cos\phi$ ) of 1 and a minimum power factor (PF) of 0.9, which is equivalent to the neutral power factor value.

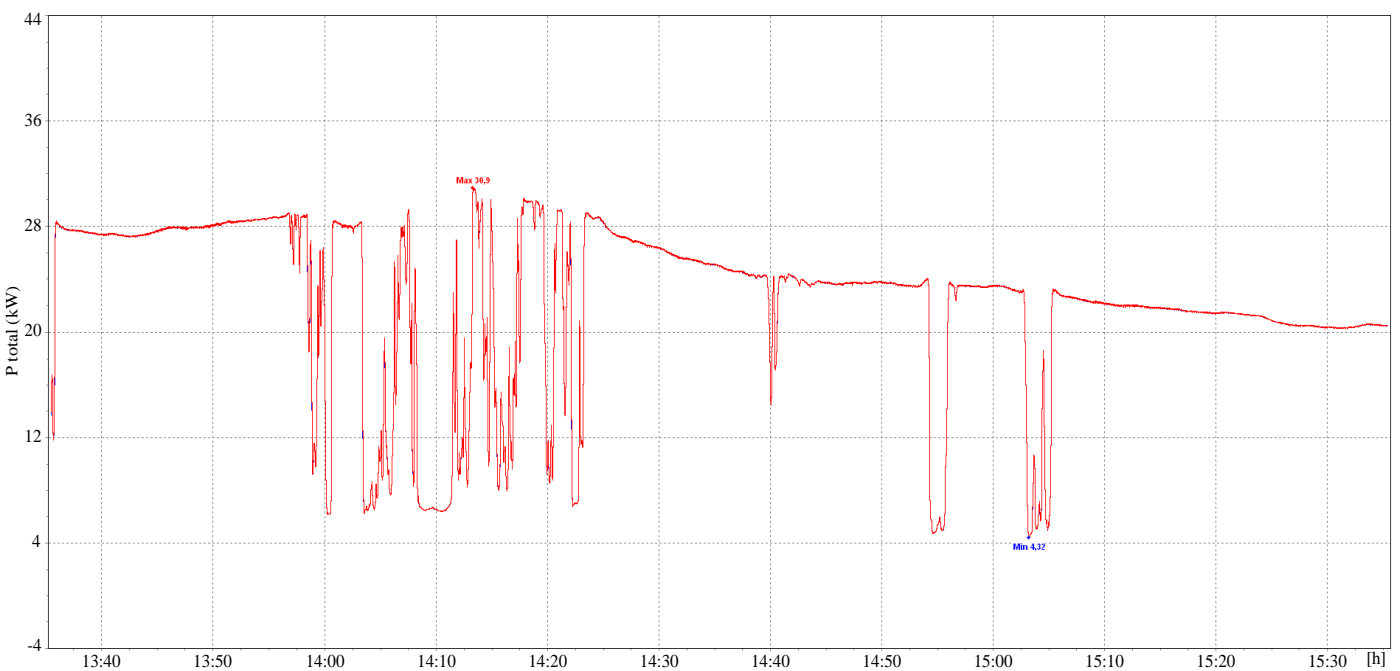


**Figure 9.** The variation mode of the power supplied by the 40 kW PV system.

The frequency variation mode of the 40 kW PV system’s supply voltage is depicted in **Figure 10**, and the minimum and maximum values, representing its variation range, in relation to a 50 Hz frequency are shown within **Table 2**. The analysis indicates that it remains within the specified range of  $\pm 1\%$ .

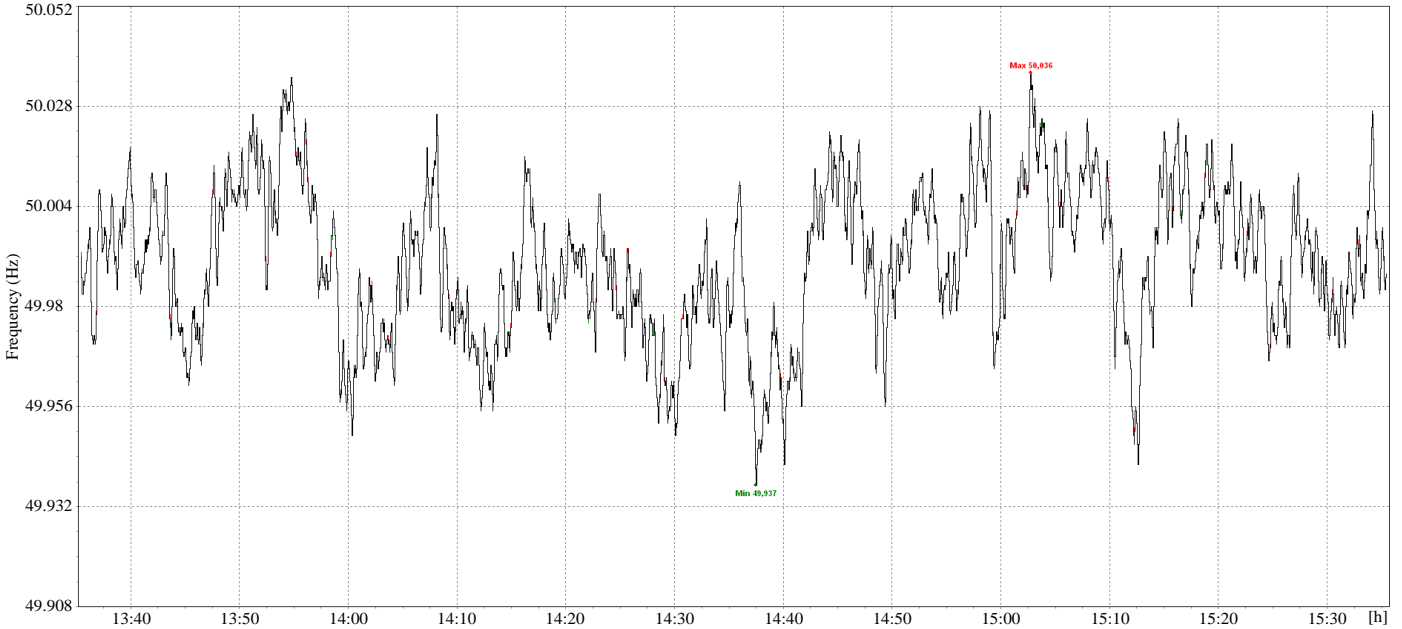


**Figure 10.** Frequency variation mode of the voltage supplied by the 40 kW PV system.

### 3.3. Analysis of the operation of the 60 kW grid-connected PV system with variable and uncontrollable load

We conducted measurements for the 60 kW PV system using the identical grid analyzer on 30.05.2024 during the time range of 12:23 ÷ 14:23. **Figure 11** illustrates the manner in which the phase voltages supplied by this system vary. **Table 3** displays the minimum and maximum voltage values for each phase, showing the range of variation compared to the standard 230 V nominal voltage.

**Table 3.** Electrical values measured on the 60 kW PV system.

Measured electrical size	Phase R/General			Phase S			Phase T		
	Min.	Max.	$\epsilon V\%$	Min.	Max.	$\epsilon V\%$	Min.	Max.	$\epsilon V\%$
Phase voltage [V]	226.4	239.5	-1.55/+4.1	228.4	241.8	-0.71/ +5.1	231.9	244.1	+6.1
Phase currents [A]	8.1	73.2	-	8.3	73.5	-	8.3	73.3	-
Frequency	49.937	50.035	$\epsilon f: -0.126\%/+0.07\%$						

It has been observed that there are larger discrepancies in the maximum voltage values for the S and T phases. When looking at the actual voltage values averaged over 10 minutes, the analysis of the data revealed the following: phase R—238.4 V (+3.6%), phase S—240.8 V (+4.7%), phase T—243.1 V (+5.7%). It is evident that the voltage on phase C falls short of meeting the required standards, the relative deviations being greater than  $\pm 5\%$ . The average voltage values for the phases during the analyzed period were: phase R—234.3 V, phase S—236.7 V, phase T—239.2 V.

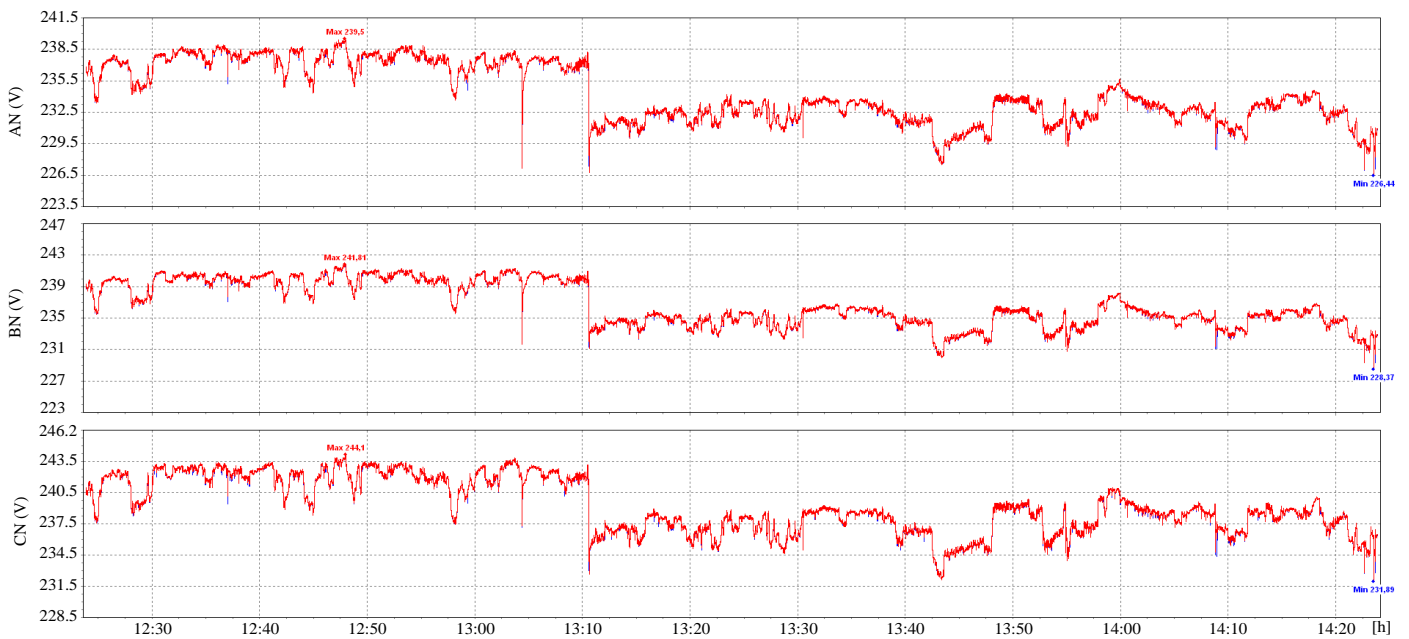


**Figure 11.** The variation mode of phase voltages provided by the 60 kW PV system.

**Figure 12** illustrates the fluctuation of currents across the three phases at the 60 kW PV system’s output, with the range displayed in **Table 3**. The symmetry of the three currents, each varying by approximately 65 A, is evident.

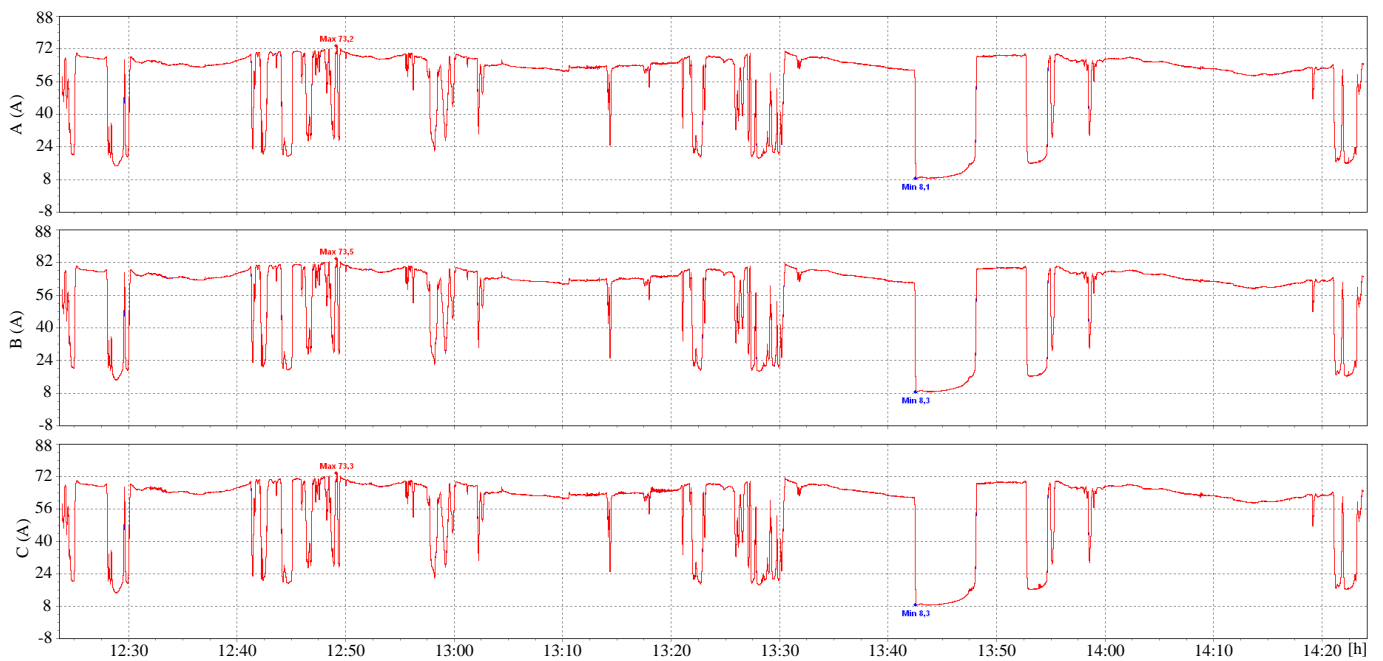


**Figure 12.** The variation mode of currents in the three power phases of the 60 kW PV system.

The power supplied by the 60 kW PV system varies in mode as depicted in **Figure 13**. The range of variation is from 5.64 kW to 52.86 kW, representing up to 88% of the PV system’s installed power. Furthermore, we have determined from the data that  $\cos\phi$  has a value of 1 and the mini-mum PF value is 0.94, indicating a power factor above the neutral point.

The frequency variation mode illustrated in **Figure 14** depicts the fluctuations

over the two-hour recording period. Upon analysis, it was observed to fluctuate between 49.939 Hz and 50.041%, equivalent to a range of  $-0.122\%$  to  $+0.082\%$  of the standardized frequency. This demonstrates that the frequency variation meets the required quality standards.

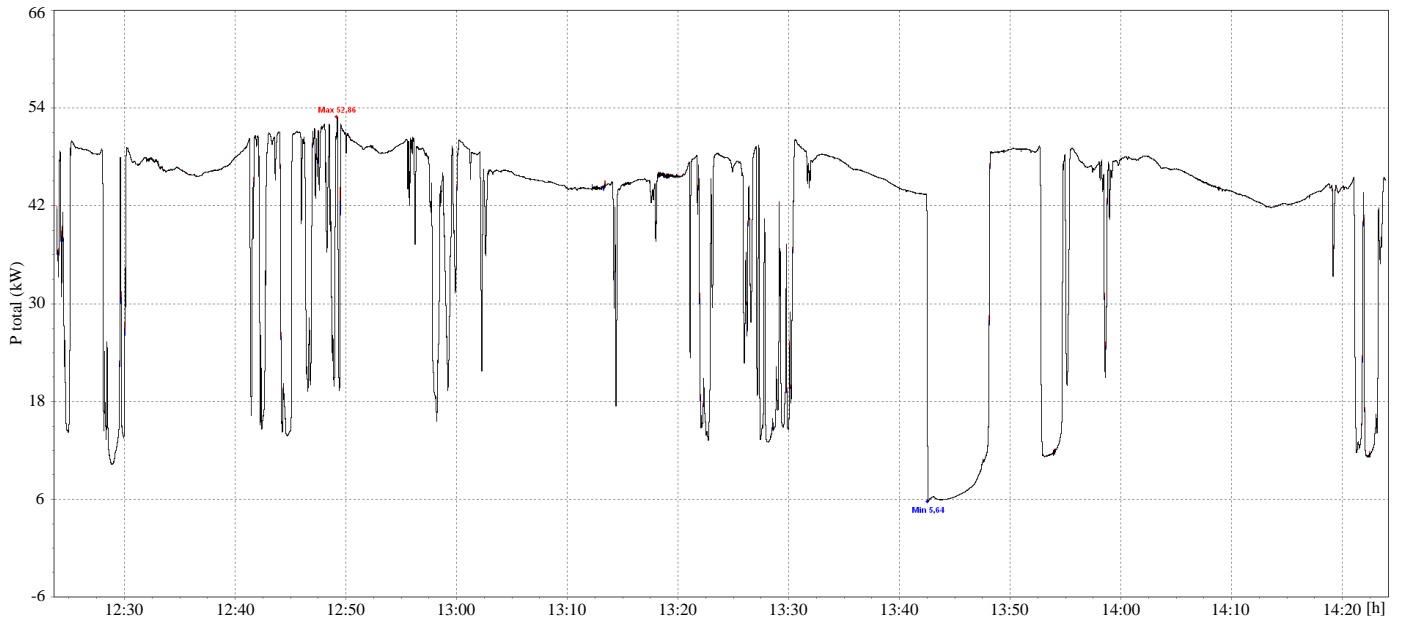


**Figure 13.** The variation mode of the power provided by the 60 kW PV system.



**Figure 14.** Frequency variation mode of the voltage supplied by the 60 kW PV system.

In summary, the 25 kW and 40 kW PV systems have voltages that deviate from the standard value by over  $\pm 5\%$ , therefore failing to meet quality standards.

#### **4. Analysis of the operation of the hybrid plant in the transient regime caused by the disconnection and reconnection of the supply**

## grid

In order to analyze this regime, commonly found in hybrid plant operation, we utilized the same network analyzer to analyze the fluctuations in voltages, currents, frequency, and active power.

To analyze the operation of the hybrid plant, a specific operating scenario was carried out:

- The consumer gets electricity from both the PV system and the grid;
- When the grid supply is cut off, a transient regime arises until the consumer receives power from the PV system and the diesel generator set, which is synchronized with the PV system;
- After the grid voltage returns, a transient regime occurs until the consumer continues to be powered by both the PV system and the grid.

We utilized the identical grid analyzer to analyze the operation, positioned between the transformer post and the automation, protection, and control system.

The variation mode of phase voltages during the analysis period on 03.06.2024 from 15:59 to 16:09 is depicted in **Figure 15**.

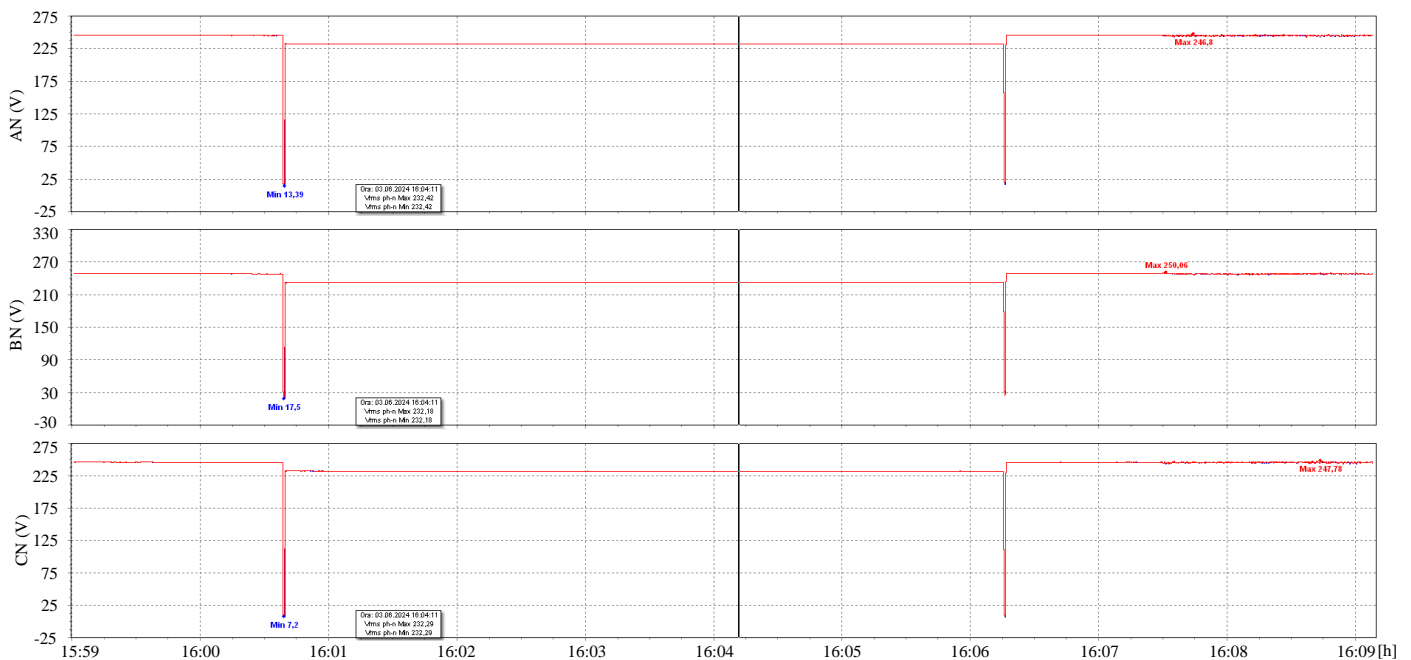


**Figure 15.** The variation mode of phase voltages provided by the 60 kW PV system.

At 16:00:38 when the power supply from the grid was interrupted there was a transient regime that lasted one second. Within this period, the phase voltages decreased (reaching a minimum value of 7.2 V on phase *T*), the diesel generator set started running and synchronized with the PV system. Upon stabilization, it supplied phase voltages of about 232 V.

At 16:06:15, the grid was reconnected, during which the diesel generator set was taken offline and the PV system was synchronized with the grid. Throughout this brief one-second period, phase voltage values decreased, reaching a minimum of 7.21 V on phase *T*.

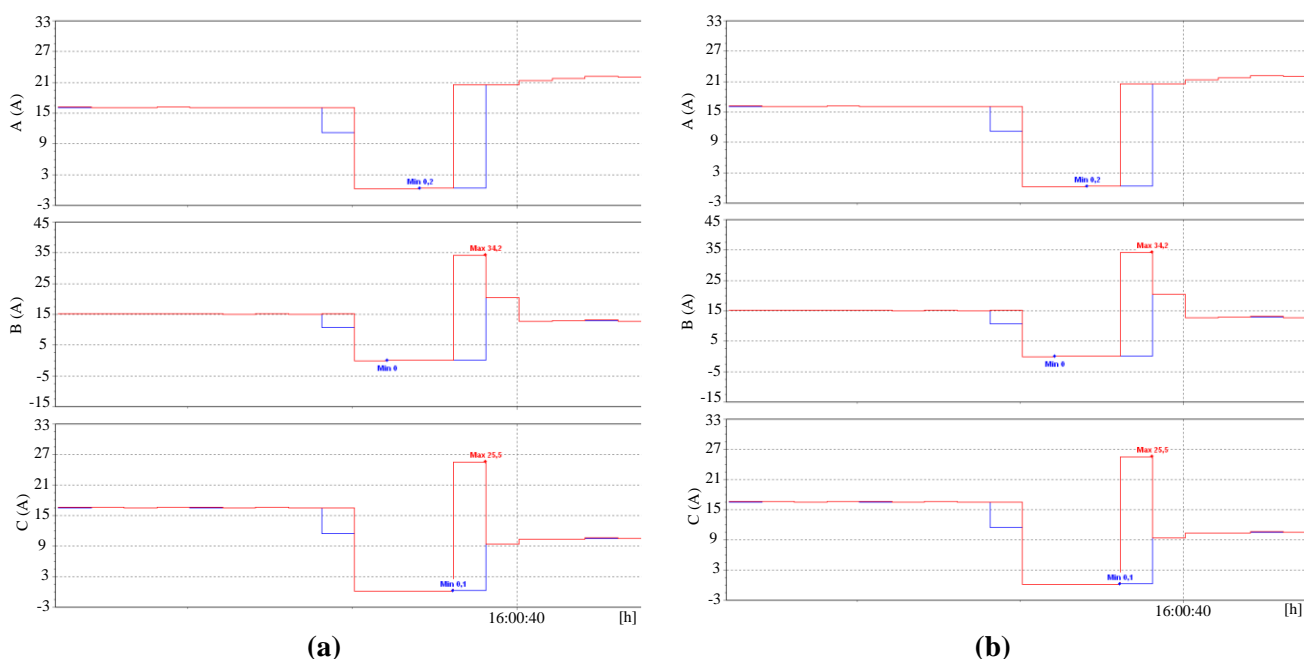


**Figure 16.** The variation mode of currents under transient regimes. **(a)** grid disconnection; **(b)** grid reconnection.

In **Figure 16a**, we have presented the variations in currents during the transient regime caused by the grid disconnection and the activation of the diesel-generator set, while in **Figure 16b**, we have illustrated the changes in currents during the transient regime resulting from the re-turn of grid voltage and the automatic disconnection of the diesel-generator set.

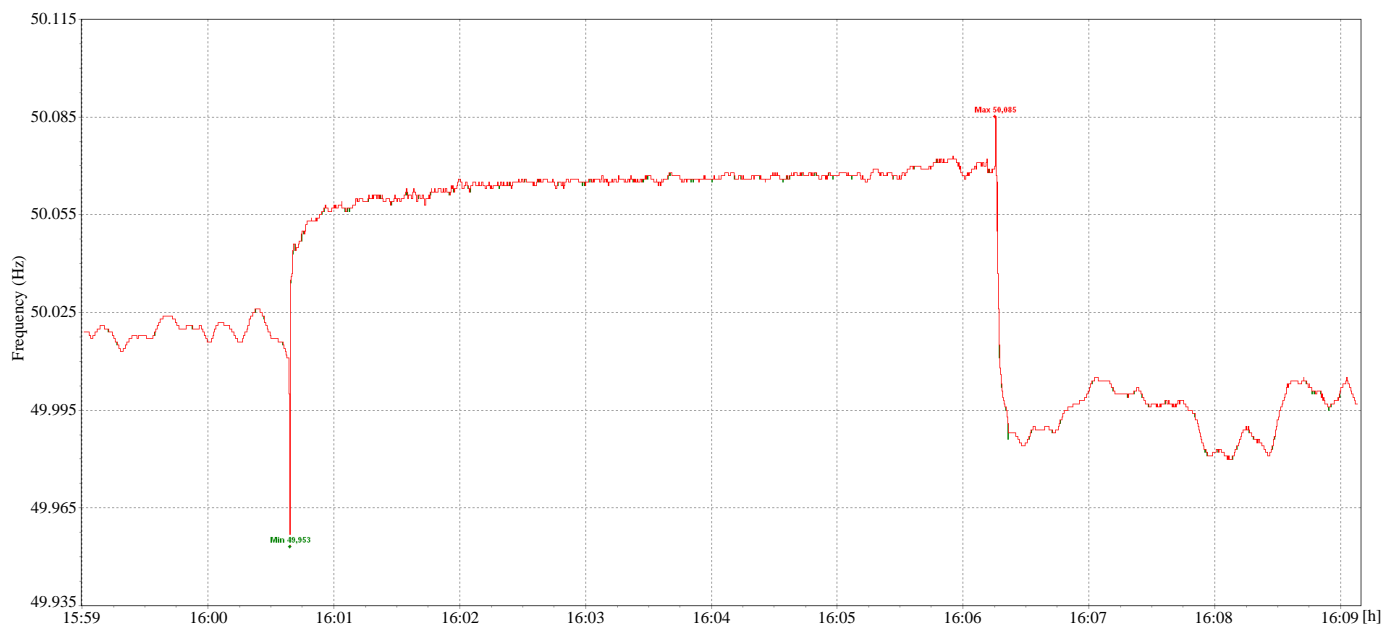


**Figure 17.** Frequency variation mode over the period of recorded transient regimes.

**Figure 17** illustrates the fluctuation in supply voltage frequency throughout the analyzed transient regimes. The analysis indicates that in the absence of grid voltage, the frequency dropped to 49.953 Hz ( $-0.094\%$  of the nominal frequency  $f_n$ ) and upon the return of grid voltage, it rose to 50.085 Hz ( $+0.17\%$  of  $f_n$ ). Consequently, the



standards for voltage frequency in supply are also satisfied during transient regimes.

During the period when the consumer was supplied power from both the PV system and the diesel generator set, the frequency variation was observed to be minimal, with the generator effectively maintaining system stability. This observation aligns with findings from other studies indicating that a hybrid PV-gas generator system provides voltage and frequency levels that fall within the acceptable operating range as well (Budiyanto et al., 2020; Priolkar and Doolla, 2016).

In **Figure 18** we presented the active power variation during the transient regimes studied. It was observed that at the time of grid connection, a peak power of 40.56 kW was injected into the grid while the consumer utilized power from the photovoltaic system synchronized with the diesel-generator set. Simultaneously, the maximum power taken from the grid was 19.32 kW.

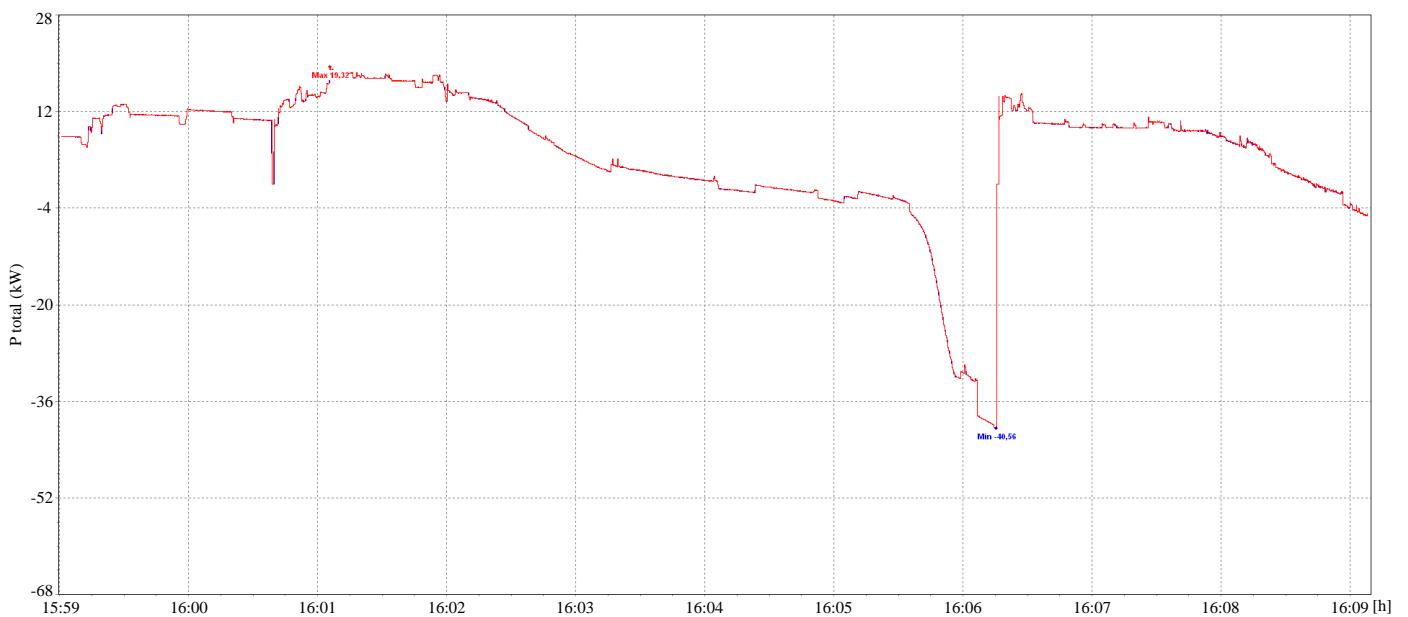


**Figure 18.** The variation mode of active power during the recorded transient regimes.

## 5. Conclusion

The hybrid power system's performance was determined by examining the voltage and frequency variation modes, both during the PV system's on-grid operation and the transient regimes of grid disconnection and reconnection.

Upon examining the magnitudes recorded for the three PV systems, it was discovered that the minimum phase voltages on the *R* and *T* phases exceeded the standard values. Specifically, for the 25 kW PV system, 95% of the actual values averaged over a 10-minute interval showed increases of +6.3% on the *R* phase, +6% on the *S* phase, and +7% on the *T* phase. For the 40 kW PV system, the voltages of the three phases had minimum values above the standard 230 V. When considering the average values over a 10-minute period, 95% of them showed increments of +6.6% on phase *R*, +6.8% on phase *S*, and +7.5% on phase *T*. In the case of the 60 kW PV system, it was observed that the minimum voltage surpassing the standard value occurred only on phase *C*. Looking at the actual voltage readings averaged over 10 minutes, 95% of them displayed increases of +3.6% on phase *R*, +4.7% on phase *S*, and +5.7% on phase *T*.

When analyzing the frequency variation due to uncontrolled changes in load and power from photovoltaic systems, it is observed that there is no significant alteration. The limit values remain within the regulatory limits ( $\pm 1\%$ ), despite the discovery of a permanent dynamic.

The conducted analysis revealed a minor imbalance in current values due to diverse loads on phases and the nature of consumers (capacitive or inductive). This loading also results in a slight imbalance in the voltage readings at the outputs of the three photovoltaic systems.

Furthermore, no significant variations were identified in the power quality issue of the hybrid system analyzed during transient regimes resulting from grid disconnection and reappearance of grid voltage.

The hybrid plant under analysis is a highly efficient plant that demonstrates good responsiveness to temporary conditions. When combined with the consumer plant, the analyzed plant can tolerate minor modifications to enhance its performance and meet all quality standards. The research's novelty lies in the experimental analysis of the hybrid plant's behavior during transient regimes, which are often overlooked in the implementation of such systems.

This article offers a new perspective on the functioning of hybrid systems through showcasing outcomes from an experimental study conducted through measurements. Utilizing modern tools for acquiring and logging electrical data enables a thorough examination of various systems' operations. Based on these analyses, potential enhancements for the system's configuration and performance optimization can be suggested.

The conventional way of analyzing the operation of hybrid systems is largely done by simulations based on implemented mathematical models. Once these systems are put into operation, the actual outputs, such as how the system operates over time, are studied without any data recordings in various operating conditions. This approach fails to capture the detailed phenomena that occur, particularly during transient regimes, which may affect specific system parts or various consumer devices. We believe that only by examining the recorded data from a hybrid system, we can accurately assess its performance under both steady-state and dynamic modes. Ongoing research aims to identify and implement measures to control voltages from grid-connected photovoltaic systems, aiming to keep voltage deviations within  $\pm 5\%$ . Simultaneously, efforts are being made to ensure continuous power supply to critical receivers during the analyzed transient regimes.

**Author contributions:** Conceptualization, SE and MGS; methodology, SE; validation, SE and SNI; formal analysis, MM; investigation, SE, MGS and SNI; resources, SE and SNI; data curation, SNI; writing—original draft preparation, MM; writing—review and editing, SE; visualization, MGS and SNI; supervision, SE; project administration, SE, SNI and MM; funding acquisition, SE, SNI and MM. All authors have read and agreed to the published version of the manuscript.

**Funding:** This research was funded by Babe Bolyai University, contract no. 36314/24.11.2023. The publication of this article was supported by the 2023 Development Fund of the UBB.

**Conflict of interest:** The authors declare no conflict of interest.

## References

- Ameen, A. M., Pasupuleti, J., & Khatib, T. (2015). Replacement model for hybrid Photovoltaic/Diesel generator/Battery system's components with typical control strategy. In: Proceedings of the 2015 IEEE Student Conference on Research and Development (SCORED). <https://doi.org/10.1109/scored.2015.7449328>
- Atănăsoae, P., Pentiuc, R. D., Milici, D. L., et al. (2019). The Cost-Benefit Analysis of the Electricity Production from Small Scale Renewable Energy Sources in the Conditions of Romania. *Procedia Manufacturing*, 32, 385–389. <https://doi.org/10.1016/j.promfg.2019.02.230>
- Averbukh M. A., Zhilin E. V., & Prokopishin, D. I. (2018). Electric Power Loss Minimization in Power Supply Systems for the Suburban Houses. *Problemele Energeticii Regionale*, 2, 31–38. <https://doi.org/10.5281/zenodo.1343394>
- Babatunde, O. M., Munda, J. L., & Hamam, Y. (2020). A Comprehensive State-of-the-Art Survey on Hybrid Renewable Energy System Operations and Planning. *IEEE Access*, 8, 75313–75346. <https://doi.org/10.1109/access.2020.2988397>
- Badea, G., Felseghi, R. A., Raboaca, M. S., et al. (2016). Techno-economical Analysis of Hybrid PV-WT-Hydrogen FC System for a Residential Building with Low Power Consumption. *Problemele Energeticii Regionale*, 3, 78–84.
- Brahim, B. (2019). Performance investigation of a hybrid PV-diesel power system for remote areas. *International Journal of Energy Research*, 43(2), 1019–1031. <https://doi.org/10.1002/er.4301>
- Budiyanto, A., Kamil, M. I., Aryani, D. R., et al. (2020). Performance analysis of a hybrid natural gas generator/photovoltaic system for residential use. *IOP Conference Series: Earth and Environmental Science*, 599(1), 012018. <https://doi.org/10.1088/1755-1315/599/1/012018>
- Chindris, M., Cziker, A., Anca, M., et al. (2016). Small Distributed Renewable Energy Generation for Low Voltage Distribution Networks. *Problemele Energeticii Regionale*, 2, 11–21.
- Coban, H. H. (2023). Hydropower Planning in Combination with Batteries and Solar Energy. *Sustainability*, 15(13), 10002. <https://doi.org/10.3390/su151310002>
- Das, D., Chakraborty, I., Bohre, A. K., et al. (2024). Sustainable Integration of Green Hydrogen in Renewable Energy Systems for Residential and EV Applications. *International Journal of Energy Research*, 2024, 1–20. <https://doi.org/10.1155/2024/8258624>
- Dehghani, F., & Shafiyi, M. A. (2023). Integration of hybrid renewable energy sources with the power system considering their economic complementarity. *IET Renewable Power Generation*, 17(15), 3638–3650. <https://doi.org/10.1049/rpg2.12871>
- EN. (1999). Voltage characteristics of electricity supplied by public distribution systems. Available online: <https://fs.gongkong.com/files/technicalData/201110/2011100922385600001.pdf> (accessed on 2 June 2024).
- Fluke. (2024). Fluke 434-II and 435-II Power Quality and Energy Analyzers. Available online: <https://www.fluke.com/en-us/product/electrical-testing/power-quality/434-435> (accessed on 24 June 2024).
- Giraud, F., & Salameh, Z. M. (2007). Measurements of Harmonics Generated by an Interactive Wind/Photovoltaic Hybrid Power System. *Electric Power Components and Systems*, 35(7), 757–768. <https://doi.org/10.1080/15325000601175132>
- Halabi, L. M., Mekhilef, S., Olatomiwa, L., et al. (2017). Performance analysis of hybrid PV/diesel/battery system using HOMER: A case study Sabah, Malaysia. *Energy Conversion and Management*, 144, 322–339. <https://doi.org/10.1016/j.enconman.2017.04.070>
- Huang, X. J., & Bao, N. S. (2017). Modeling and simulation analysis of wind-hydro hybrid power plant. In: Proceedings of the 2nd Annual International Conference on Energy, Environmental & Sustainable Ecosystem Development (EESD 2016). <https://doi.org/10.2991/eesd-16.2017.22>
- IEC. (2015). Testing and measurement techniques—Power quality measurement methods. Available online: <https://webstore.iec.ch/en/publication/21844> (accessed on 2 June 2024).
- Isakov, I., & Todorovic, I. (2021). Power production strategies for two-stage PV systems during grid faults. *Solar Energy*, 221, 30–45. <https://doi.org/10.1016/j.solener.2021.03.085>
- Kemp, J. M., Millstein, D., Kim, J. H., et al. (2023). Interactions between hybrid power plant development and local transmission in congested regions. *Advances in Applied Energy*, 10, 100133. <https://doi.org/10.1016/j.adapen.2023.100133>
- Khosravani, A., Safaei, E., Reynolds, M., et al. (2023). Challenges of reaching high renewable fractions in hybrid renewable energy systems. *Energy Reports*, 9, 1000–1017. <https://doi.org/10.1016/j.egyr.2022.12.038>

- Manoj, D., Tomonobu, S., Atsushi, Y., et al. (2011). A Frequency-Control Approach by Photovoltaic Generator in a PV-Diesel Hybrid Power System. *IEEE Transactions on Energy Conversion*, 26(2), 559–571. <https://doi.org/10.1109/tec.2010.2089688>
- Maritz, J., Gorjão, L. R., Bester, P. A., et al. (2024). Data-Driven Modeling of Frequency Dynamics Observed in Operating Microgrids: A South African University Campus Case Study. *IEEE Access*, 12, 14466–14473. <https://doi.org/10.1109/access.2024.3357945>
- Martínez, J., & Medina, A. (2010). A state space model for the dynamic operation representation of small-scale wind-photovoltaic hybrid systems. *Renewable Energy*, 35(6), 1159–1168. <https://doi.org/10.1016/j.renene.2009.11.039>
- Mthwecu, S., & Chowdhury, S. (2015). Solar PV/Diesel Hybrid Power System design using macroeconomic analysis. In: *Proceedings of the 2015 50th International Universities Power Engineering Conference (UPEC)*. <https://doi.org/10.1109/upec.2015.7339958>
- Neamt, L., Petrean, L., Chiver, O., et al. (2018). Some Considerations About Overvoltages During and After the Disconnection of a Photovoltaic Park. In: *Proceedings of the 2018 IEEE 24th International Symposium for Design and Technology in Electronic Packaging (SIITME)*. <https://doi.org/10.1109/siitme.2018.8599251>
- Nguyen, H. V. P., Nguyen, V. T., Vo, Q. S., et al. (2021). Enhancing effectiveness of grid-connected photovoltaic systems by using hybrid energy storage systems. *Journal of Engineering Science and Technology*, 16(2), 1561–1576.
- ANRE. (2021). Performance standard for electricity distribution service. *Official Monitor*, 649(1).
- Pan, W., Gao, W., & Muljadi, E. (2009). The dynamic performance and effect of hybrid renewable power system with diesel/wind/PV/battery. In: *Proceedings of the 2009 International Conference on Sustainable Power Generation and Supply*. <https://doi.org/10.1109/supergen.2009.5348178>
- Priolkar, J. G., & Doolla, S. (2013). Analysis of PV-hydro isolated power systems. In: *Proceedings of the 2013 Annual IEEE India Conference (INDICON)*. <https://doi.org/10.1109/indcon.2013.6725890>
- Ratnata, I. W., Sumarto, S., & Saputra, W. S. (2019). Performance analysis of Pico Hydro-Solar Photovoltaic Hybrid System. In: *Proceedings of the 2nd International Symposium on Materials and Electrical Engineering (ISMEE)*; 17 July 2019; Bandung, Indonesia.
- Siddaraj, U., & Tangi, S. (2016). Integration of DG systems composed of photovoltaic and a micro-turbine in remote areas. In: *Proceedings of the 2016 International Conference on Computation of Power, Energy Information and Commuincation (ICCPEIC)*. <https://doi.org/10.1109/iccpeic.2016.7557332>
- Spunei, E., Piroi, I., & Piroi, F. (2022). Efficiency of a small power photovoltaic installation connected to the low voltage network. *Journal of Physics: Conference Series*, 2212(1), 012020. <https://doi.org/10.1088/1742-6596/2212/1/012020>
- Spunei, E., Piroi, I., Piroi, F., et al. (2021). Examining the Performances of a Low Power Photovoltaic Installation. In: *Proceedings of the 2021 12th International Symposium on Advanced Topics in Electrical Engineering (ATEE)*. <https://doi.org/10.1109/atee52255.2021.9425231>
- Zhang, Y., Ma, C., Yang, Y., et al. (2021). Study on short-term optimal operation of cascade hydro-photovoltaic hybrid systems. *Applied Energy*, 291, 116828. <https://doi.org/10.1016/j.apenergy.2021.116828>